Fermi surface topology and low-lying quasiparticle dynamics of parent $Fe_{1+x}Te/Se$ Superconductor by orbital-polarization resolved ARPES

Y. Xia,[1] D. Qian,[1,2] L. Wray,[1,3] D. Hsieh,[1] G.F.
Chen,[4] J.L. Luo,[4] N.L. Wang,[4] and M.Z. Hasan[1,5,6]

[1]*Joseph Henry Laboratories of Physics, Department of Physics,*
Princeton University, Princeton, NJ 08544

[2]*Department of Physics, Shanghai Jiao Tong University, Shanghai 200030, China*

[3]*Lawrence Berkeley National Laboratory,*
University of California, Berkeley, CA 94305

[4]*Beijing National Laboratory for Condensed Matter Physics,*
Institute of Physics, Chinese Academy of Sciences, Beijing, China

[5]*Princeton Center for Complex Materials,*
Princeton University, Princeton, NJ 08544

[6]*Princeton Institute for the Science and Technology of Materials,*
Princeton University, Princeton, NJ 08544

(Dated: June 30, 2009)

Abstract

We report the first photoemission study of $Fe_{1+x}Te$ - the host compound of the newly discovered iron-chalcogenide superconductors (maximum $T_c \sim 27K$). Our results reveal a pair of nearly electron-hole compensated Fermi pockets, strong Fermi velocity renormalization and an absence of a spin-density-wave gap. A shadow hole pocket is observed at the "X"-point of the Brillouin zone which is consistent with a long-range ordered magneto-structural groundstate. No signature of Fermi surface nesting instability associated with $Q=(\pi/2, \pi/2)$ is observed. Our results collectively reveal that the $Fe_{1+x}Te$ series is dramatically different from the high T_c pnictides and likely harbor unusual mechanism for superconductivity and magnetic order.

PACS numbers:

The discovery of superconductivity in the pnictides (FeAs-based compounds) has generated interest in understanding the general interplay of quantum magnetism, electronic structure and superconductivity in iron-based layered compounds [1, 2]. The recent observation of unusual superconductivity and magnetic order in the structurally simpler compounds such as FeSe and $Fe_{1+x}Te$ are the highlights of current research [3, 4, 5, 6, 7]. The expectation is that these compounds may provide a way to isolate the key ingredients for superconductivity and the nature of the parent magnetically order state which may potentially differentiate between vastly different theoretical models [8, 9, 10]. The crystal structure of these superconductors comprises of a direct stacking of tetrahedral FeTe layers along the c-axis bonded by weak van der Waals coupling. Superconductivity with transition temperature up to 15K is achieved in the $Fe_{1+x}(Se,Te)$ series [3, 4] and T_c increases up to 27K under a modest application of pressure [5]. Density functional theories (DFT) predict that the electronic structure is very similar to the iron-pnictides and magnetic order in FeTe originates from very strong Fermi surface (FS) nesting leading to the largest SDW gap in the series. Consequently, the doped FeTe compounds are expected to exhibit T_c much higher than that observed in FeSe if superconductivity would indeed be originating from the so called $(\pi,0)$ spin fluctuations [10]. These predictions critically base their origin on the Fermi surface topology and the band-structure details, however, no experimental results on the Fermiology and band-structure exist on this sample class to this date. Here we report the first angle-resolved photoemission spectroscopy (ARPES) study of the $Fe_{1+x}Te$ - the host compound of the superconductor series. Our results reveal a pair of nearly electron-hole compensated Fermi pockets, significant band renormalization and a remarkable absence of the predicted large SDW gap. Although the observed Fermi surface topology is broadly consistent with the DFT calculations, no Fermi surface nesting instability associated with the magnetic ordering wave vector was observed. An additional hole pocket is observed in our data which can be interpreted to be associated with a local-moment magneto-structural groundstate in clear contrast to inter-band nesting. Our measurements reported here collectively suggest that the FeTe compound series is dramatically different from the parent compound of the pnictide superconductors and may harbor novel forms of magnetic and superconducting instabilities not present in the high T_c pnictides.

Single crystals of $Fe_{1+x}Te$ were grown using the Bridgeman technique. A mixture of grounded Fe and Te powder was heated to 920°C in an evacuated tube then slowly cooled,
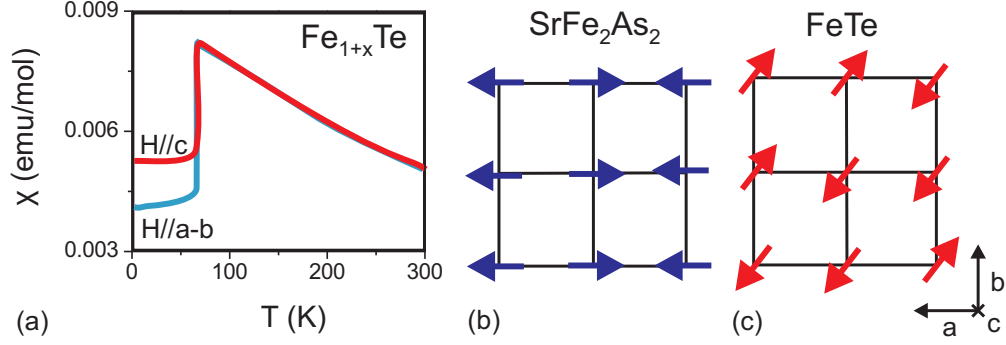
FIG. 1: Magneto-structural transition and long-range order in Fe_{1+x}Te: (a)Temperature dependence of the magnetic susceptibility [6]. (b) The spins in $SrFe_2As_2$ are collinear and $\mathbf{Q}_{AF}$ points along the $(\pi, 0)$ direction. (c) The ordering vector, $\mathbf{Q}_{AF}$ in FeTe, is rotated by $45°$ and points along the $(\frac{\pi}{2}, \frac{\pi}{2})$ direction [15].

forming single crystals. The iron concentration was measured by inductively-coupled plasma technique and x was determined to be less than 0.05. High-resolution ARPES measurements were then performed using linearly-polarized 40eV photons on beamline 10.0.1 of the Advanced Light Source at the Lawrence Berkeley National Laboratory. The energy and momentum resolution was 15meV and 2% of the Brillouin Zone (BZ) using a Scienta analyzer. The in-plane crystal orientation was determined by Laue x-ray diffraction prior to inserting into the ultra-high vacuum measurement chamber. The magnetic order below 65K was confirmed by DC susceptibility measurements (Fig-1). The samples were cleaved *in situ* at 10K under pressures of less than 5×10^{-11} torr, resulting in shiny flat surfaces. Cleavage properties were characterized by STM topography and by examining the optical reflection properties.

Figure 2 presents the momentum dependence of the photoemission intensity n(k) at 10K at various binding energies (0, -20, -40 and -60 meV), integrated over an energy window of $\pm$ 5 meV at each binding energy. The non-zero spectral intensity at the Fermi level (μ) confirmed that the low temperature state of Fe_{1+x}Te is metallic-like. At the Fermi level, electrons are mostly distributed in one broad hole-like pocket at Γ and another similar size electron-like pocket around M. To reveal the band shapes we present a gradual binding-energy evolution of the band features and present the data in a way to simulate the effect of rigidly lowering of the chemical potential down to 60meV. The FS (at 0 meV) is seen
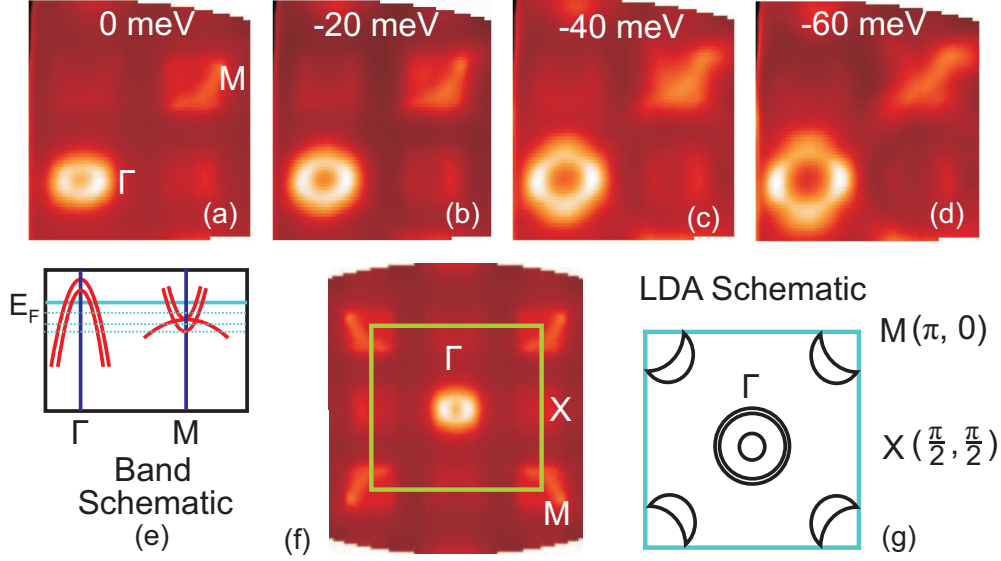
FIG. 2: **Fermi surface topology**: (a) Fermi surface topology of FeTe. (a-d) Connection to the underlying band-structure is revealed by considering the evolution of the density of states, n(k), as the chemical potential is rigidly lowered by 20, 40 and 60 meV. The Fermi surface consists of hole pockets centered at Γ, and electron pockets centered at M. An additional hole-like feature is observed at M in (b-d), which is attributed to a band lying below E_F (see schematic in (e)). (e) presents a schematic of the band dispersions in the Γ-M direction forming the observed electron and hole pockets. A qualitative agreement is observed between the (f) the experimentally measured FS topology and (g) the LDA calculated [10] FS although measured bands are strongly renormalized.

to consist of circular hole pockets centered at Γ, and elliptical electron pockets at the M points. An elliptical-like feature at the M point expands as the binding energy is increased, suggesting that the associated band is hole-like. We will subsequently show that this band lies below μ and the M-point Fermi pockets are only electron-like (2(e)). By considering the dominant intensity patterns in panel-(a-d), apart from a weak feature at "X"-point, the FS topology is similar to that expected from the DFT calculations (2(g)) [10]. In addition, the area of the hole-like FS pocket at Γ and the electron-like FS pocket at M are approximately equal in size suggesting nearly equal number of electron and hole carrier densities in this material. Therefore, if the excess Fe atoms are contributing to the carrier density it is likely to be small and beyond our k-resolution of the experiment.

In order to systematically study the low lying energy band structure, ARPES spectra are taken along different k-space cut directions in the 2D Brillouin zone (BZ). Two different

electron-photon scattering geometries are used to ensure that all bands are imaged. In a σ scattering geometry, where the polarization vector is along k_y and the detector slit is along k_x, photoelectron signal is predominantly from the d_{xy} and d_{yz} energy bands due to the dipole emission matrix elements [11, 12]. Similarly, when the detector slit is along k_y, the π-geometry, the d_{xz}, d_{z^2} and $d_{x^2-y^2}$ states are predominantly excited. Figure 3 (a) and (b) present scans along the $\Gamma - M$ direction in the σ and π geometries. In both sets of spectra, one finds a broad hole-like band centered at Γ. However, near M the scans taken at two different geometries are drastically different. In cut 1, two hole-like bands (α_2, α_3 as marked in panel (a)) are observed to be approaching μ. Under the π geometry the band emission pattern near M is dramatically different (see the β_1 band in cut 2), while the α_2 and α_3 band signals are significantly weaker. The polarization dependence suggests that the β_1 band should have d_{xz}, d_{z^2}, or $d_{x^2-y^2}$ orbital character.

In order to fully resolve the broad band feature centered at Γ, high resolution scans are performed along different k-cut directions through the zone center. Figure 3(c) presents one cut in the $\Gamma - M$ direction inside the first zone, together with the corresponding energy distribution curve (EDC). Two hole-like bands are resolved, labeled α_2 and α_3. Since there are traces of multiple bands near M, one might wonder whether the α_3 band crosses μ near the M point, thus forming a hole-like Fermi pocket. To systematically investigate this, a series of spectra are taken along the $\Gamma - M$ direction with π-geometry (3(d)-(f)) through multiple k-cuts intersecting the M-point Fermi pocket. At M, cut-4 shows a strong electron-like band forming the FS pocket. This band can be attributed to the β_1 band (also observed in cut-2). As one moves away from M, the band intensity becomes increasingly more hole-like, indicating the emergence of the α_2 band. Nevertheless, the hole band lies completely and consistently below the Fermi level, with some weak electron quasiparticle intensity above the band maximum. The β_1 intensity becomes the weakest near the edge of the M pocket (cut-6). But even at that location, the hole pocket lies at least 10meV below the chemical potential. The result shows that there are no hole pocket features in the FS near M which supports the interpretation that this material is nearly electron-hole compensated. Additionally, one can map the observed bands to the band structure estimated by DFT calculations (schematic in 3(g) [10]). The calculation finds three bands (α_1-α_3) crossing Fermi level near Γ and two (β_1, β_2) near M, forming the electron and hole pockets. While the DFT calculated bands agree fairly well with our data, within our resolution or
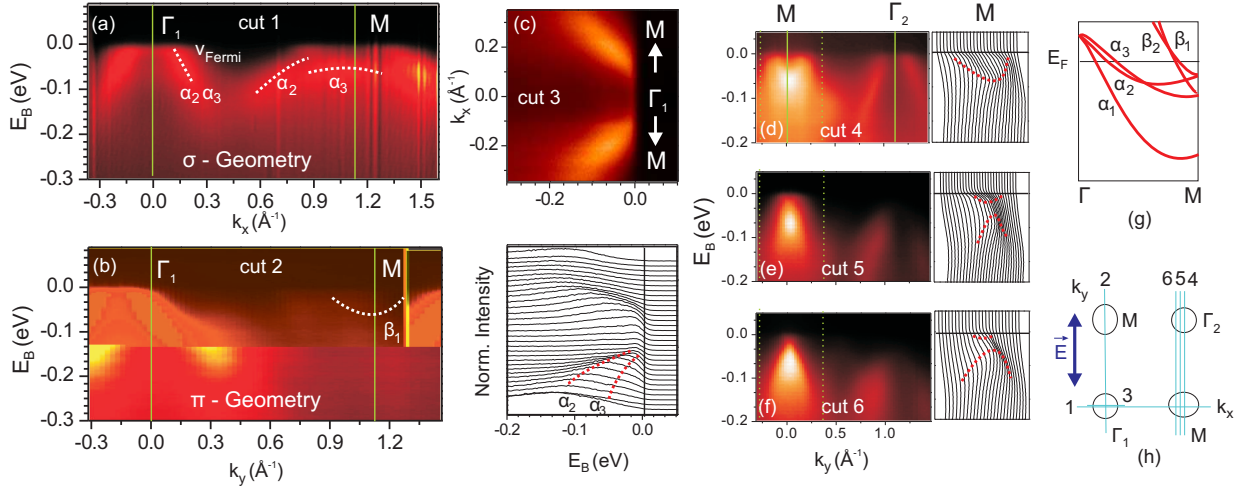
FIG. 3: **Low-lying band topology**: ARPES spectra along the $\Gamma - M$ direction in the (a)σ and (b)π-scattering geometries. v_F of the quasiparticle band forming the Γ hole pocket is calculated from the dashed line. (c) The EDC of a high momentum resolution scan through Γ shows two hole-like bands crossing the E_F. (d)-(f) Cuts along the M-Γ direction through the electron FS pocket show that the hole band near M remains at least 10meV below E_F. For each scan direction the corresponding EDC is also presented, within the momentum range marked by green dashed lines. Comparison with (g) a band dispersion schematic of the LDA result [10] shows a good agreement between experiment and theory. (h) The directions of the six scans are summarized and identified in the first BZ. The direction of the electric field is shown.

the sample surface roughness, we have not succeeded in fully resolving the α_1 band near Γ. The β_2 band, which forms the second M electron pocket, is observed in the Fermi surface topology (Fig. 2). The overall band narrowing is about factor of 2 compared to the DFT calculations highlighting the importance of correlation effects. This is also consistent with a small Fermi velocity ($v_{Fermi} \sim 0.7$ eV·$\mathring{A}$) observed (Fig.3(a)).

We now revisit the details of the FS map (Fig.-2) and discuss a weak feature observed at X=$(\frac{\pi}{2}, \frac{\pi}{2})$ between two Γ points (Fig. 4(e)). Such a feature is not expected from the DFT calculations. A similar feature, whose origin is debated, has been observed in AFe$_2$As$_2$ (**A**=Ba, Sr), which is attributed to a 2×1 surface reconstruction of the **A** atom layer [13, 14], in addition to a weak bulk structural distortion. However, in FeTe there are no additional atoms (such as Sr or Ba) between the Fe layers and the crystal cleaves at a weak van der
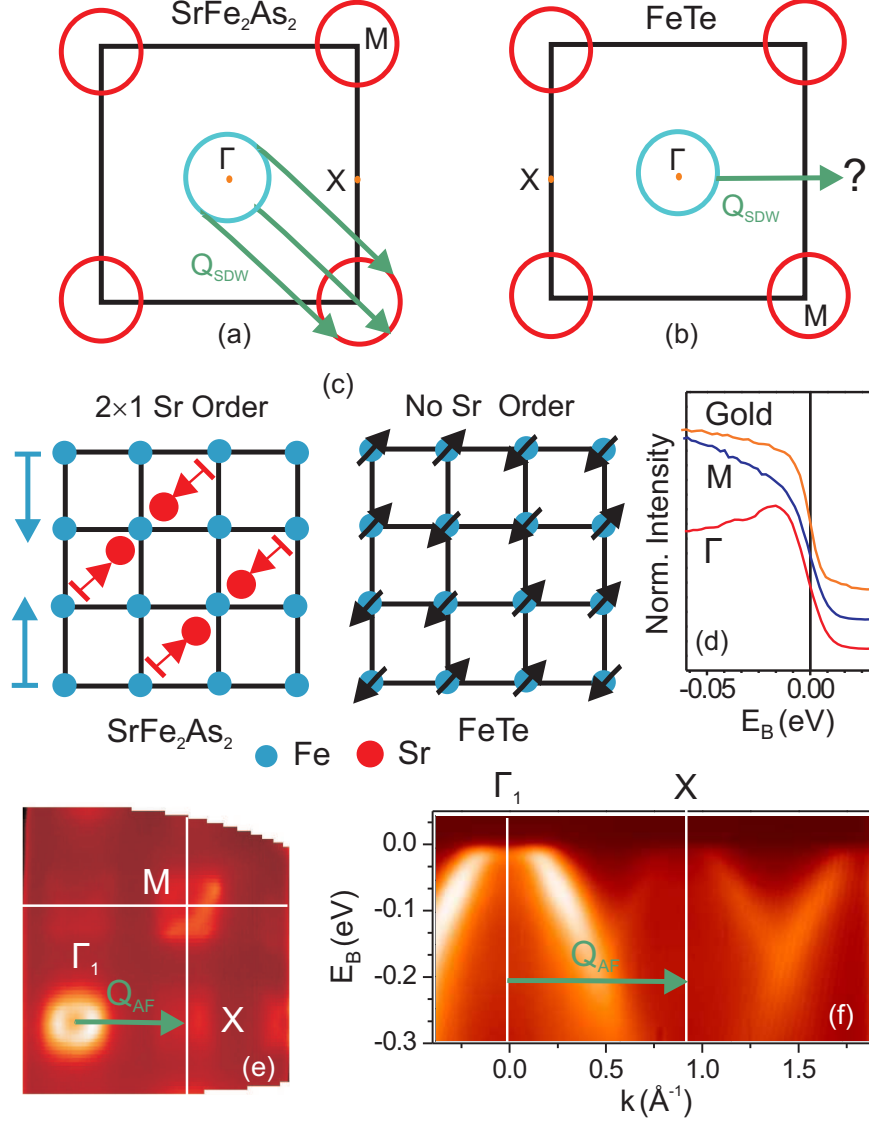
FIG. 4: **Electronic structure and Magnetism**: While (a) the electron and hole pockets in SrFe$_2$As$_2$ can be kinematically nested by $\mathbf{Q}_{AF}$=(π,0), there exists (b) no FS pocket which can be nested by $\mathbf{Q}_{AF} = (\frac{\pi}{2}, \frac{\pi}{2})$ in the FeTe BZ. A FS pocket observed at X in SrFe$_2$As$_2$ has been attributed to the (c) 2×1 surface order of the Sr atomic layer (red), which occurs in addition to a weak bulk distortion (blue) across the SDW transition. However, there are no additional Sr atoms between the Fe layers in FeTe, so no Sr order is possible, although a weak bulk distortion is not excluded. (d) The EDCs measured at near the Γ and M pockets exhibit no evidence of energy gaps. Nevertheless, (e) a weak FS pocket is observed at X, (f) corresponding to two hole-like bands dispersing towards the chemical potential which is consistent with a long-range local moment magneto-structural order.

Waals bond between two adjacent layers. Therefore, no strong 2×1 long-range ordered **A**-type reconstruction is expected except for a weak bulk-like structural orthorhombicity tied to the magnetic order (magneto-structural effect). Recent neutron [15, 16] and x-ray diffraction [17, 18] studies have shown that FeTe undergoes a bulk structural distortion from the tetragonal to weakly-monoclinic or orthorhombic phase near 65K, accompanied by long-range magnetic order $Q_{AF}=(\frac{\pi}{2}, \frac{\pi}{2})$.

In the parent compound of the pnictide superconductors such as the $SrFe_2As_2$ or $BaFe_2As_2$, the SDW vector $\mathbf{Q}_{SDW} =(\pi, 0)$ coincides with a Fermi surface nesting vector connecting the hole-pocket at Γ and the electron pocket at M. Currently, it is believed that this nesting is responsible for opening a gap in the low temperature physical properties [6, 11, 19]. In the case of FeTe, while a nesting vector can indeed be drawn along $\mathbf{Q}_{SDW} =(\pi, 0)$ between a pair of electron and hole pockets, all available neutron scattering measurements report that the antiferromagnetic ordering vector is 45° away from that in $SrFe_2As_2$, namely, in $Fe_{1+x}Te$, $\mathbf{Q}_{AF} =(\frac{\pi}{2}, \frac{\pi}{2})$. The ordering shows a commensurate to incommensurate cross-over if the concentration of excess iron, x, is increased. Another remarkable difference is that the magnetic susceptibility is Curie-Weiss like in FeTe suggesting that the magnetism is of local-moment origin. Within a local moment-like AFM long-range ordered state which also couples to a weak structural distortion one should expect relatively intense shadow Fermi surfaces along the Neel vector $\mathbf{Q}_{AF}$. The X-point Fermi surface we observe thus can be related to the vector observed in neutron scattering $X = \Gamma+\mathbf{Q}_{AF}$. The weak shadow-like X pocket FS might therefore arise from a band folding due to long-range magnetic order. However, unlike $SrFe_2Se_2$, where the Γ electron pocket nests with the M hole pockets via $\mathbf{Q}_{SDW} = (\pi, 0)$ [20], an analogous nesting channel is unavailable at $(\frac{\pi}{2}, \frac{\pi}{2})$ in the FeTe (4(b)) clearly ruling out FS nesting as the origin of magnetic order. In the absence of nesting FS gapping is not expected in FeTe which is consistent with our results in Fig-2 and 3. A large low temperature specific heat value [6] is thus consistent with our observation of a Fermi surface in the correlated magneto-structurally ordered state. To examine the band dispersion character of the X pocket, figure 4 (f) presents a spectra along the $\Gamma - X$ direction. Results show two bands dispersing towards μ, forming the hole pocket in the "X"-FS whose shapes are indeed very similar to the bands that form the central Γ-pocket FS. Further evidence against nesting comes from the absence of a large gap at the overall low temperature electron distributions presented in Fig-2 and 3 (4(d)). Our results seem to

suggest that the groundstate is a nearly electron-hole compensated semimetal. Absence of a gap is consistent with recent bulk optical conductivity, specific heat and Hall measurements in FeTe [6] (while most measurements do report a gap in $SrFe_2As_2$ [19]).

A recent density functional calculation [21] suggests that the excess Fe is in a valence state near Fe^+ and therefore donates electron to the system. Due to the interaction of the magnetic moment of excess Fe with the itinerant electrons of FeTe layer a complex magnetic ordering pattern is realized. In this scenario, excess Fe would lead to an enlargement of the electron pocket FS, however, within our resolution electron and hole Fermi surface pockets are measured to be of very similar in size suggesting a lack of substantial electron doping due to excess Fe. Finally, we note that a gapless yet long-range ordered local-moment magneto-structural groundstate consistent with ARPES and neutron data taken together is captured in both first-principles electronic structure [8] and many-body spin model [9] calculations. However, the broad agreement of DFT calculations with experimental band-structure data except for about a factor 2 renormalization is also remarkable. A complete understanding of electron correlation, moment localization and the true nature of the gapless antiferromagnetic state would require further systematic ARPES study.

In conclusion, we have presented the first ARPES study of Fermi surface topology and band structure of $Fe_{1+x}Te$. Our results reveal a pair of *nearly* electron-hole compensated Fermi pockets, significant renormalization and the remarkable absence of a spin-density-wave gap. The observed shadow hole pocket is consistent with a long-range ordered local moment-like magneto-structural groundstate whereas, most remarkably, no Fermi surface nesting instability associated with the antiferromagnetic order was observed. Contrary to band theory suggestions [22], results collectively suggest that the $Fe_{1+x}Te$ series is different from the undoped phases of the high T_c pnictides and likely harbor a novel mechanism for superconductivity and quantum magnetism.

and materials growth supported by NSFC and CAS China (NLW).

---

[1] Y. Kamihara, T. Watanabe, M. Hirano, and H. Hosono, J. Am. Chem. Soc. **130**, 3296 (2008); Z.A. Ren *et al.*, Chin. Phys. Lett. **25**, 2215 (2008).

[2] G.F. Chen *et al.*, Phys. Rev. Lett. **100**, 247002 (2008); X. H. Chen *et al.*, Nature **453**, 761 (2008).

[3] F.C. Hsu *et al.*, Proc. Natl. Acad. Sci. **105**, 14262 (2008).

[4] M.H. Fang *et al.*, Phys. Rev. B **78**, 224503 (2008).

[5] Y. Mizuguchi *et al.*, Appl. Phys. Lett. **93**, 152505 (2008).

[6] G.F. Chen *et al.*, arXiv:0811.1489 (2008).

[7] C. Xu and S. Sachdev, Nature Phys. **4**, 898 (2008).

[8] F.J. Ma *et al.*, arXiv:0809.4732 (2008).

[9] C. Fang *et al.*, arXiv:0811.1294 (2008).

[10] A. Subedi *et al.*, Phys. Rev. B **78**, 134514 (2008).

[11] D. Hsieh *et al.*, arXiv:0812.2289 (2008).

[12] D. Qian *et al.*, Phys. Rev. Lett. **97**, 186405 (2006).

[13] M.C. Boyer *et al.*, arXiv:0806.4400 (2008).

[14] Y. Yin *et al.*, arXiv:0810.1048 (2008).

[15] S. Li *et al.*, arXiv:0811.0195 (2008).

[16] W. Bao *et al.*, arXiv:0809.2058 (2008).

[17] K. Yeh *et al.*, arXiv:0808.0474 (2008).

[18] Y. Mizuguchi *et al.*, arXiv:0810.5191 (2008).

[19] W.Z. Hu *et al.*, Phys. Rev. Lett. **101**, 257005 (2008).

[20] J. Zhao *et al.*, Phys. Rev. B **78**, 140504 (2008).

[21] L. Zhang *et al.*, arXiv:0810.3274 (2008).

[22] M. Johannes, Physics **1**, 28 (2008)